First-principles calculation of the three-dimensional band structure of poly(phenylene vinylene)

P. Gomes da Costa
Center for Photoinduced Charge Transfer, University of Rochester, Rochester, New York 14627 and Xerox Webster Research Center, Webster, New York 14580

R. G. Dandrea
Xerox Webster Research Center, Webster, New York 14580

E. M. Conwell
Center for Photoinduced Charge Transfer, University of Rochester, Rochester, New York 14627 and Xerox Webster Research Center, Webster, New York 14580

(Received 2 July 1992)

We have carried out a local-density-functional calculation of the three-dimensional (3D) band structure of the conducting polymer poly(phenylene vinylene) (PPV). The motivation was to investigate the effects of interchain coupling. The major effects are due to coupling of carbons in the rings to their closest neighbors, hydrogens on rings in adjacent chains. Among the effects of this coupling are splitting by up to 0.4 eV at various points of the Brillouin zone of the double degeneracy that would exist if the two chains in the unit cell were uncoupled; loss of electron-hole symmetry; the band edge at a point in the Brillouin zone off the chain direction; and a band gap smaller by 0.2 eV than that obtained from 1D calculations. The calculation results in a ratio of the transfer integral $t_\perp$ perpendicular to the chains to $t_\parallel$, parallel to the chains, $\simeq 0.03$. This value is too large to permit the existence of polarons in a perfect PPV crystal. Nevertheless, there is evidence for the existence of polarons in PPV crystals currently available. The large value of $t_\perp/t_\parallel$ means that polaron existence must be due to defects, such as inclusions of precursor polymer. This would result in the polarons having a wide range of properties, i.e., extent on the chain and energy levels.

I. INTRODUCTION

Poly(phenylene vinylene) (PPV) is a conjugated polymer whose repeat unit, shown in Fig. 1,[1] consists of a vinyl group, similar to the repeat unit of polyacetylene, plus a phenyl ring. The properties of PPV have been much studied, particularly since it was found to be electroluminescent,[2] thus presumably a candidate for large area displays. Single-chain, or one-dimensional (1D) band structures have been calculated.[3–5] The calculations reported here give the first 3D band structure.

Although polymers such as PPV may be synthesized with chains well aligned so that they are highly anisotropic, there is mounting evidence of many kinds that 3D effects such as interchain interactions cannot be neglected. According to a 1D treatment, an electron or hole added to a polymer chain causes relaxation of that chain. For PPV, a polymer with a nondegenerate ground state, the resulting excitations would be polarons and bipolarons with wave functions quite extended along the chain. The existence of bipolarons in PPV is well documented. They occur in samples doped with a few percent or more of donor or acceptor impurities. Direct evidence for the bipolarons is the very low electronic contribution to the magnetic susceptibility of these samples, indicating that the electron spins are paired.[6] It has also been shown that steady-state photoexcitation with the electric vector perpendicular to the chains results in bipolaron creation.[7–9] With polarization perpendicular to the chains, the electron and the hole may be created on separate chains, avoiding the formation of an exciton and allowing the electron or hole to subsequently find another electron or hole, respectively, to make up a bipolaron.

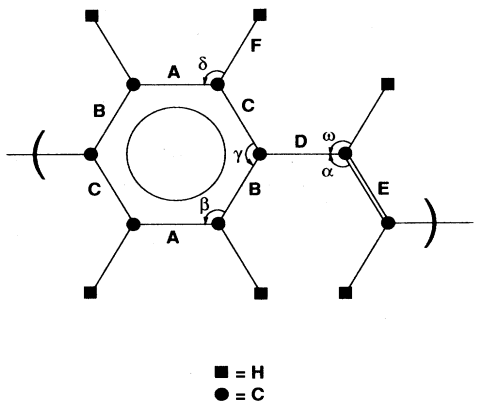

FIG. 1. Repeat unit (monomer) of PPV. From Ref. 1, $A=B=C=1.39$ Å, the single bond $D=1.44$ Å, while the double bond $E=1.33$ Å, $F=1.09$ Å, $a=128°$, $\beta=\gamma=\delta=120°$, $\omega=116°$. The circle inside the ring indicates the resonant structure, with the π electrons delocalized throughout the ring.

According to the 1D model, an isolated electron or hole on a chain would form a polaron extended over several monomer units. It has been pointed out, however, that, unless interchain coupling is quite weak, such a polaron is unstable.[10,11] Calculations of Vogl and Campbell, based on the local-density-functional 3D band structure of polyacetylene obtained by them,[12,13] show that the polaron is indeed unstable in that case. They point out, however, that their calculation is done for a perfect lattice, and disorder could stabilize the polaron.[11] The stability of polarons in PPV has already been questioned on the basis of electroluminescence measurements.[14]

In Sec. II of this paper we describe the structure of PPV as determined by x rays. Section III is devoted to the self-consistent solution of the Kohn-Sham equations, using nonlocal pseudopotentials to remove the core electrons of carbon from the problem. In Sec. IV we present the resulting electronic band structures for the case of one chain per unit cell and for the actual case of two chains per unit cell. If the structure of PPV were perfect, it would have one of two possible space-group symmetries, $P2_1/a$ or $P2_1/n$. As will be shown, these differ in the relative location of the repeat unit on nearest-neighbor chains. We have carried out our calculations for both of these symmetries. Finally, in Sec. V we summarize our results, returning to the question of the stability of the polaron.

II. CRYSTAL STRUCTURE OF PPV

As noted earlier, the vinyl group of PPV is quite similar in structure to the repeat unit of polyacetylene. The single bond D shown in Fig. 1 is 0.01 Å shorter than the single bond in polyacetylene, while the double bond E is 0.03 Å shorter than the double bond in that case.[15] The experimental values of D and E are within ~ 0.01 Å of the values calculated for PPV using MNDO (modified neglect of differential overlap).[15]

The experimental data on which Fig. 1 is based have all sides of the ring equal in length, 1.39 Å. MNDO gives lengths for the sides of the ring within 0.01 Å of this value,[15] but shows the rings to be slightly quinoid with $A < B$ or C by 0.01 Å. We have neglected this difference.

In Fig. 1, the ring is taken to be in the plane of the backbone. More recent analyses of x-ray-diffraction data show the rings to be at a small angle, $\sim 7°-10°$ for different samples, to the backbone.[16] This twist of the rings is due to the repulsive interaction between the H's on the ring and those on the vinyl group. Temperature studies of the diffraction show that the twist angle increases a little with temperature. Also, there is a thermally induced rotation or libration of the rings about the backbone, specifically about the axis defined by the two single bonds that connect to the rings. The maximum angular displacement due to this libration is $\sim 7°-9°$ at 300 K.[16] Incorporation of the ring rotation would double the unit cell because adjacent rings on a chain are expected to twist in opposite directions. Because of the increased computer time this would entail, most of our calculations were done for planar PPV. As will be described, a calculation we did with the rings twisted by 7° showed only small changes in the band structure.

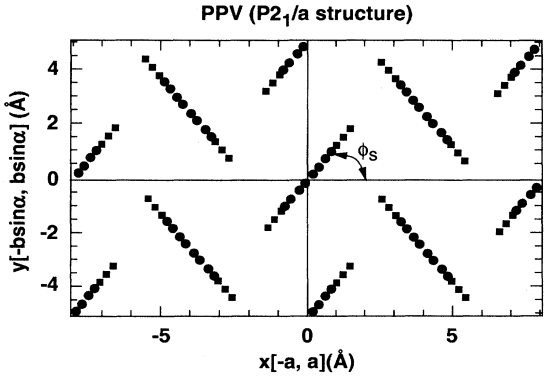

FIG. 2. Projection of unit cell perpendicular to the chain direction. Φ_s, the setting angle, is 52° (Ref. 17).

X-ray diffraction on oriented PPV samples gives the unit cell as monoclinic, containing two monomer units.[1] Thus the unit cell contains 16 carbon atoms and 12 hydrogen atoms. The most recent values of the unit-cell pa-

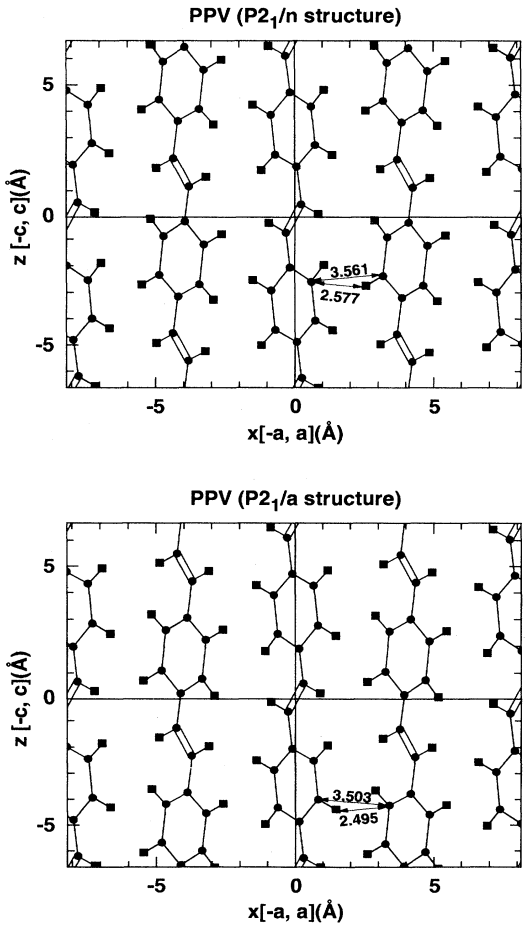

FIG. 3. Projection of $P2_1/n$ and $P2_1/a$ onto the xz (ac) plane.

rameters are $a=8.07$ Å, $b=6.05$ Å, c (chain axis)$=6.54$ Å, and a, the angle between b and c, 123°.[17] These values are close to those reported earlier.[1] The herringbone structure of the lattice is evident in Fig. 2, which shows the projection of the unit cell perpendicular to the chain direction. Chen *et al.*[17] quote a value for the setting angle Φ_s (see Fig. 2) of 52°. This value, used in our calculations, is somewhat lower than the values given by Granier *et al.*[1]

As noted earlier, if perfectly ordered, PPV would have the space group $P2_1/n$ or $P2_1/a$. Figure 3 shows the projections of $P2_1/n$ and $P2_1/a$ onto the xz (ac) plane, where it is seen that the two structures differ by a translation of adjacent chains. X rays show that there is disorder which causes the registry of adjacent chains to vary.[18]

Recent morphology studies of PPV films made from a precursor polymer and oriented by stretching show about 50% of the film to consist of small crystallites about 50 Å in size.[19] The crystallites are connected by regions in which the chains are disordered. The disordered regions are not expected to be truly amorphous because of the rigid character of the PPV chain. Neutron scattering indicates that a single chain may traverse many crystallites.[20] Given these findings, we speculate that each crystallite has a single symmetry, $P2_1/a$ or $P2_1/n$. If the difference between the energies of these two phases is quite small, as was found for polyacetylene,[13] both symmetries would be present in the films, in different crystallites.

III. COMPUTATIONS

Our calculations were performed using local-density-functional theory (LDF) (Refs. 21 and 22) and the norm-conserving pseudopotential method.[23,24] LDF theory has its source in a theorem by Hohenberg and Kohn,[21] which states that in the ground state the external potential $V_i(\mathbf{r})$ due to the ions, and therefore the total energy E and other properties of the many-electron system, are functionals of the electron density $\rho(\mathbf{r})$. Minimizing $E[\rho]$, keeping the total number of electrons N constant, one obtains the self-consistent Kohn-Sham equations[22] for the single-particle wave functions $\Psi_i(\mathbf{r})$:

$$\left[-\frac{\hbar^2}{2m_e}\nabla^2+V_i(\mathbf{r})+v_{\mathrm{Hxc}}[\rho(\mathbf{r})]\right]\Psi_i(r)=E_i\Psi_i(\mathbf{r}) ,$$

$$\rho(\mathbf{r})=e\sum_{i=1}^{N}|\Psi_i(\mathbf{r})|^2 ,$$

where $v_{\mathrm{Hxc}}[\rho(\mathbf{r})]$ is the Hartree plus exchange and correlation potentials. This equation must be solved iteratively; $\rho(\mathbf{r})$ is the only information transmitted from one step to the other of the iteration.

Because carbon is a first-row element in the Periodic Table (without a core p state to orthogonalize the $2p$ valence state) it can have a very hard p pseudopotential, meaning it requires a large plane-wave basis set for convergence. For this reason we employed the nonlocal norm-conserving ionic pseudopotential of Troullier and Martins[25] for carbon, particularly constructed to optimize the softness of the pseudopotential and thus minimize the size of the basis set needed to represent it. In the case of hydrogen we used the true $1/r$ potential.

The wave functions were expanded in plane waves[24] with kinetic energy up to 20 Ry. To test convergence with respect to the basis-set size we performed calculations on *trans*-polyacetylene, $(CH)_x$, which also has a monoclinic structure. Polyacetylene has only four atoms in the unit cell, allowing expansion of the wave functions in plane waves up to 60 Ry. The comparison between the two materials is useful because convergence is determined by the pseudopotentials and we used the same carbon and hydrogen potentials for *trans*-$(CH)_x$ as for PPV. We found that convergence of the total energy for polyacetylene requires a cutoff of 60 Ry. However, the value of the band gap is close to convergence at 20 Ry. The difference between the band gap at 60 Ry and the band gap at 20 Ry is only 0.04 eV. Thus we can say that the 20-Ry cutoff is sufficient for the calculation of electronic band structure. However, if we want to determine structural properties, complete convergence of the total ground-state energy is required, for which a cutoff of 60 Ry would be needed. The size of the matrix (15 000) for that case makes the calculation time prohibitive (using the present nonseparable pseudopotentials) even with the CRAY-YMP on which our calculations were performed.

The method of special **k** points[26] was used to perform the integrations in **k** space over the first Brillouin zone. Broyden's technique[27,28] was used to achieve self-consistency. In our calculations, the iterations were continued until the maximum difference between the input and output potentials reached 10^{-4} Ry. In a first-principles LDF calculation, the exchange-correlation potential is not an adjustable function; it is defined to be the exchange-correlation energy of a homogeneous electron gas with the local density. The function which is now widely accepted as the most accurate is the energy calculated numerically for a large range of densities by Ceperley and Alder[29] using Monte Carlo techniques. An analytic fit to these results by Perdew and Zunger[30] was used in our calculations. We calculated the total energy using the expression given by Ihm, Zunger, and Cohen.[24]

Matrix diagonalization was an important issue with the large Hamiltonian matrices encountered in our calculations. At 20 Ry the matrix size was 2735. We used a technique based on the DIIS (direct inversion in the iterative subspace) method[31] for the iterative determination of eigenvalues and eigenvectors.

IV. ELECTRONIC PROPERTIES OF CRYSTALLINE PPV

A. Charge density

Results of our calculations will be given for both $P2_1/a$ and $P2_1/n$. Although the calculations gave $P2_1/n$ slightly smaller energy, as noted earlier we have not used a large enough basis set for this result to be regarded as conclusive. In fact, as will be discussed, it might be more likely on physical grounds that $P2_1/a$ has lower total energy. In any case, the two energies do appear to be quite

close, which suggests, as indicated earlier, that at least with the synthetic methods currently used, a sample of PPV may contain some crystallites with $P2_1/a$ and some with $P2_1/n$.

As a preliminary, consider the charge density to be expected for an isolated chain of PPV. We assume the ring to be in the plane of the backbone. The wave functions may then be classified as σ or π according to whether they are symmetric or antisymmetric with respect to reflection in the plane of the backbone. Every pair of atoms, C-C or C-H, is connected by a σ bond made up of s and p orbitals in this plane. In addition, pairs of C atoms are connected by π bonds, made up of p orbitals with axes perpendicular to the plane of the backbone. The π levels have higher energy than the σ electron levels because they have an extra node. These facts underlie the Su-Schrieffer-Heeger (SSH) Hamiltonian,[32] and other Hamiltonians based on the Hückel technique, which considers only the wave functions of π electrons, the σ bonds being treated as providing elastic coupling between the C atoms. An important prediction of the SSH model and similar one-chain models is electron-hole symmetry, i.e., energy bands for $+E$ and $-E$ being the same when $E=0$ is taken at the center of the gap. The result of the LDF calculations for the total charge density in the plane of the chain backbone is shown in Fig. 4. This plot shows the strong σ bonds between each pair of atoms. The circular pattern inside the ring demonstrates the delocalization of electrons suggested in the bonding diagram, Fig. 1.

Wave functions of the uppermost valence band and the lowest conduction band are, according to the previous discussion, expected to be pure π and π^*, i.e., bonding and antibonding combinations, respectively, of carbon p orbitals directed perpendicular to the plane. Although, as will be seen, our calculations showed these wave functions to be predominantly π and π^*, it is significant that they are not entirely so, as shown in Fig. 5. The charge density of the top two valence bands does not vanish in the plane of the backbone, as it must for π symmetry, and notably, does not vanish at the H's in the ring. The reason for this is readily seen to be the interchain coupling. When the band structure is calculated with the

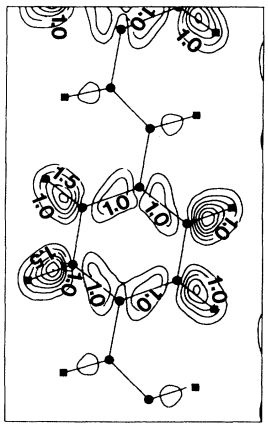

FIG. 5. Charge density in the plane of the backbone for the top two valence bands summed over the entire Brillouin zone.

chains moved away from each other by removing one chain from the unit cell and rotating the remaining chains through 27° to maximize the interchain distance, the top valence band no longer shows any charge density on the H's. As indicated in Fig. 3, the distance of closest approach between atoms on neighboring chains is 2.495 Å for a H on the ring in one chain and a C on the ring in a neighbor for the $P2_1/a$ structure, 2.577 Å for the $P2_1/n$ structure. This is similar to the situation in polyacetylene in that the closest approach there, 2.9 Å for $P2_1/a$, is between a H on one chain and a C on another chain,[12,13] but, of course, polyacetylene has no rings. It is seen in Fig. 3 that the distance between nearest-neighbor carbons on adjacent chains is ~40% larger than the smallest distance between C and H on adjacent chains. It will be shown in the next section that interchain coupling effects fall off very rapidly with distance between the atoms concerned. We conclude that the interchain coupling arises from the C-H interaction.

As found also in polyacetylene, the wave function of the two lowest conduction bands, shown in Fig. 6, is more nearly π^*, made up of essentially pure C states rather than a mixture of H and C states. Thus the interchain coupling results in an electron-hole asymmetry in the wave functions. Wave functions of the top valence

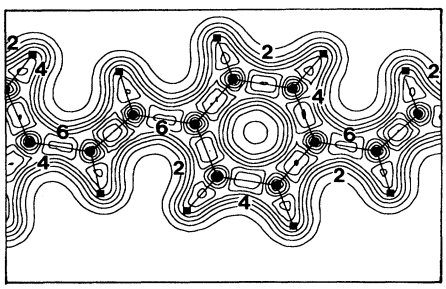

FIG. 4. Calculated valence charge density in the plane of the backbone. The straight lines joining pairs of atoms are a guide for the eye. The numbers indicate the relative charge density.

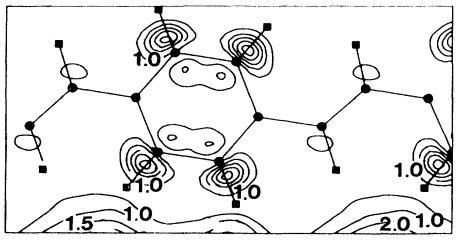

FIG. 6. Charge density in the plane of the backbone for the bottom two conduction bands summed over the entire Brillouin zone.

bands and lowest conduction bands at various points in the Brillouin zone will be shown in Sec. IV D.

B. Splitting of the electronic energy levels

The Brillouin zone of PPV is shown in Fig. 7. Although the top face in the figure looks almost hexagonal, the zone is monoclinic, as is the unit cell in the direct space. ΓP is the chain direction. Note that P is not a symmetry point of the zone. The calculated valence- and conduction-band structures for $P2_1/a$ and $P2_1/n$ are shown in Figs. 8 and 9, respectively.

The zero of the energy scale has been chosen to coincide with the highest valence-band energy. The energy gap, indicated by cross hatching, is not that calculated with LDF theory but includes a correction that will be discussed subsequently. There are 38 valence bands to accommodate the 76 electrons coming from the C and H orbitals in the unit cell. For reference we have numbered these bands 1 to 38, starting from the bottom of the valence band. Conduction bands are numbered 39,40, . . . , etc. If there were no interaction between the two chains in the unit cell, the valence- and conduction-band levels would all be doubly degenerate. It is seen, however, that there are many small splittings of the bands. This feature was also found in the LDF structure calculated for *trans*-polyacetylene.[12,13] That the splittings result from interchain interaction is shown unequivocally by a calculation of the PPV band structure with one chain removed from the unit cell and the remaining chains rotated as described previously to maximize the interchain distances. The resulting band structure is shown in Fig. 10. The splittings are absent.

The maximum splitting for $P2_1/a$ is greater than that for $P2_1/n$, 0.41 vs 0.29 eV. Thus, although the C-H distance in the $P2_1/n$ structure is only 3% larger than for $P2_1/a$, the splitting is smaller by more than 30%. This

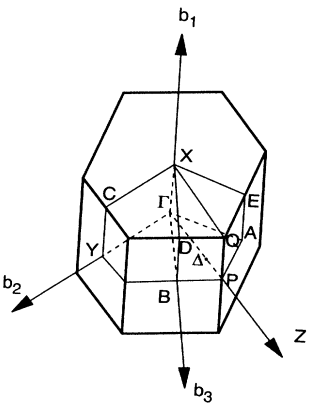

FIG. 7. Brillouin zone of PPV. ΓP is the chain direction. In terms of the reciprocal-lattice vectors $b_1(=2\pi b\times c/\Omega)$, $b_2(=2\pi c\times a/\Omega)$, and $b_3(=2\pi a\times b/\Omega)$, where $\Omega=ab\times c$, $\Gamma=(0,0,0)$, $A=(0,-\frac{1}{2},\frac{1}{2})$, $B=(0,0,\frac{1}{2})$, $C=(\frac{1}{2},\frac{1}{2},0)$, $D=(\frac{1}{2},0,\frac{1}{2})$, $E=(\frac{1}{2},-\frac{1}{2},\frac{1}{2})$, $X=(\frac{1}{2},0,0)$, $Y=(0,\frac{1}{2},0)$, and $P=(0,-0.355,0.707)$. The point $\Delta=(0,-\frac{1}{4},\frac{1}{2})$ lies on the line from Γ to P, at 0.7 of the distance from Γ to P.

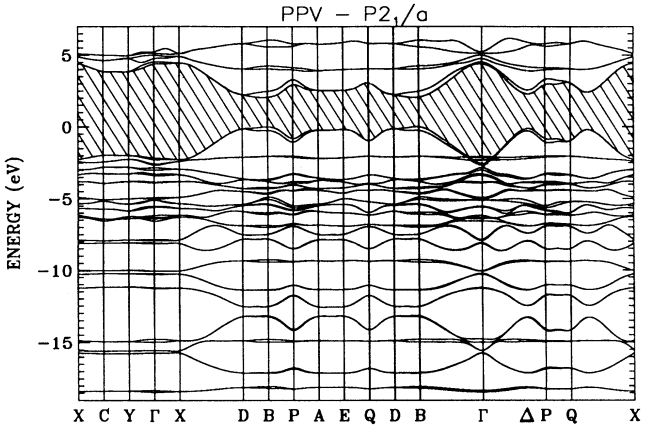

FIG. 8. Calculated energy vs wave vector for $P2_1/a$. The crosshatched region represents the energy gap.

provides the justification for neglecting the interaction of carbons on adjacent chains, for which the separation is ~40% larger than the C-H separation. We note also that the smaller C-H separation may result in $P2_1/a$ having somewhat lower total energy than $P2_1/n$, as was found for *trans*-polyacetylene.[13]

The maximum splitting of 0.410 eV in $P2_1/a$ is found for the conduction band No. 39 at point B. At that point the valence-band splitting is 0.249 eV, making the average splitting 0.330 eV. We take that figure as a measure of the interchain coupling strength for $P2_1/a$. In the simple tight-binding model that is widely used, the coupling strength between neighbors on adjacent chains is characterized by a transverse bandwidth $4t_\perp$. Taking the average splitting at B as $4t_\perp$, we obtain $t_\perp=0.082$ for $P2_1/a$. For $P2_1/n$ the maximum splitting occurs at the **k** point A, as was also the case for polyacetylene.[12] Averaging

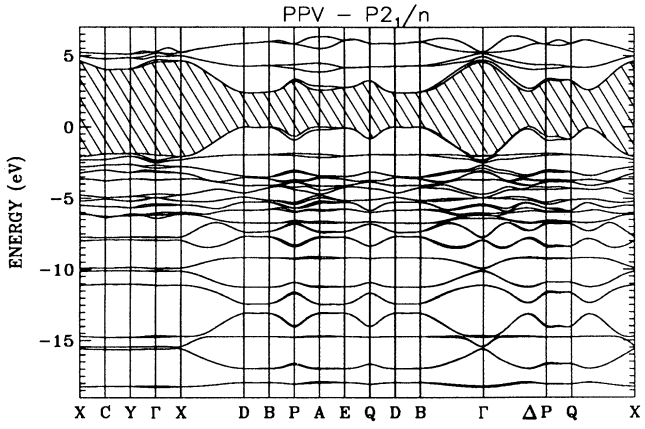

FIG. 9. Calculated energy vs wave vector for $P2_1/n$. The crosshatched region represents the energy gap.

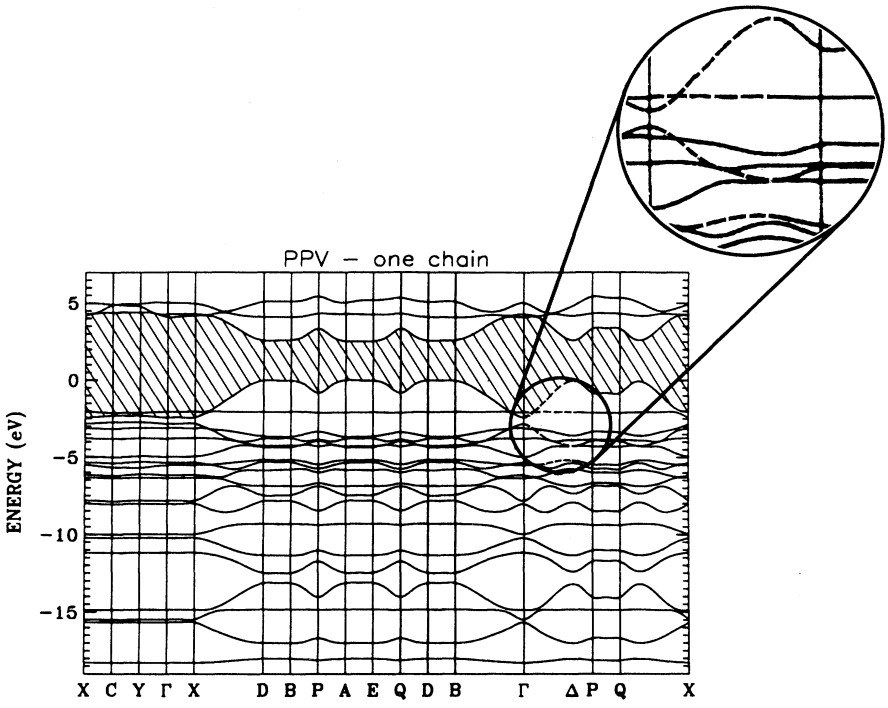

FIG. 10. Calculated energy vs wave vector for much greater spacing between the chains. The π bands are indicated by dashed lines.

conduction- and valence-band splitting at A, we obtain 0.244 eV, from which $t_\perp = 0.061$ for $P2_1/n$. As anticipated, $t_\perp$ is smaller for $P2_1/n$ than for $P2_1/a$ because of the greater interchain C-H distance.

Another significant feature of the 3D band structure is the lack of electron-hole symmetry. The band structure of Fig. 10, calculated as discussed with much greater separation between the chains, is close to showing symmetry about the middle of the gap. As anticipated earlier, the lack of electron-hole symmetry is due to the interaction between the H's and C's on different chains.

C. Band edges and gap

Band-structure calculations using density-functional theory have the shortcoming of underestimating the energy gap in semiconducting phases. The difficulty stems from the disparity between the density-functional exchange-correlation potential and the true quasiparticle self-energy. The true conduction band differs from that calculated with LDA by a self-energy term that varies somewhat with wave vector,[33–35] typically by as much as some tenths of an eV. As is frequently done, we have chosen to correct the error in the conduction-band energies by an upward shift independent of **k**. That shift was chosen to bring the band gap into agreement with the measured gap. We take the measured gap to be 2.4 eV, the value measured by optical absorption.[15]

Because the $P2_1/n$ and $P2_1/a$ structures differ very little, we estimate that the difference in the self-energy corrections for the two should be <0.02 eV. We have therefore, in obtaining Figs. 8 and 9, taken the corrections for the two to be the same. Inspection of Fig. 8, and an enlarged version of part of it, Fig. 11, suggests

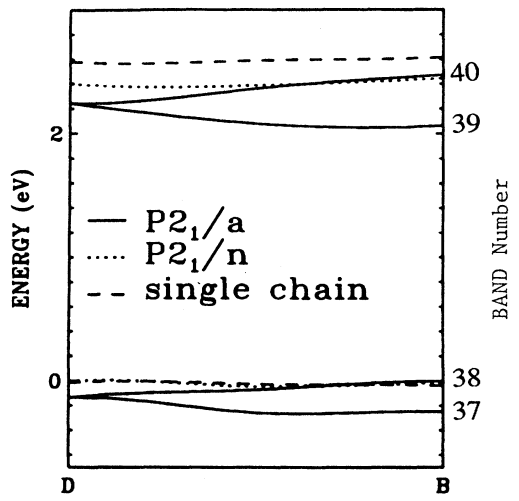

FIG. 11. A magnified view of bands 37–40 from D to B. Bands 39 and 40 have been corrected by an upward shift of 1.26 eV for $P2_1/a$, $P2_1/n$ and the "single chain" cases.

that the minimum gap for P_{2_1}/a is at or near B, between two splitoff bands Nos. 38 and 39. A calculation of the matrix element at B for an optical transition showed it to be very small, however, for transitions between bands 38 and 39, as well as between Nos. 37 and 40. For the other two possible transitions at B the matrix element was four or more orders of magnitude larger. Thus the lowest optical transition for P_{2_1}/a would be between bands 37 and 39. With a correction of 1.26 eV this leads to an optical gap of 2.35 eV and a thermal gap smaller by ~ 0.3 eV. The minimum gap calculated for P_{2_1}/n before correction, which occurs at a point between B and D, was 1.19 eV. For P_{2_1}/n, the bands are not split in this region of the zone and the optical matrix element is large. With a correction of 1.26 eV the optical gap for P_{2_1}/n becomes 2.45 eV.

It is seen from Figs. 8 and 9 that the gaps at Δ are almost the same as those in the neighborhood of B and D. Specifically, for P_{2_1}/a with the correction of 1.26 eV the optical gap at Δ, between bands 37 and 39, is 2.59 eV. (The gap between bands 38 and 40 is larger by 0.12 eV.) Whether the difference of 0.24 eV found between the optical gap at Δ and that near B is significant depends clearly on how $\mathbf{k}$ dependent is the correct shift of the conduction-band levels. For typical zinc-blende semiconductors the difference in the shift between different minima is found, by comparison of LDF results with experiment, to be ~ 0.3 eV. However, in contrast to the zinc-blende case, where the wave functions of different minima are different, the wave functions at B, D, and Δ are essentially the same. We therefore estimate the magnitude of the $\mathbf{k}$ dependence of the correction to be no more than 0.1 eV. As a result, we conclude that the band edge for P_{2_1}/a is at or near B, not at Δ. For P_{2_1}/n the optical gap at Δ, between bands 37 and 39, is also found to be 0.2 eV higher than that between B and D. Thus the band edge in the 3D case lies between B and D, having a wave vector that is off the chain direction. We have also concluded that P_{2_1}/a has a thermal gap smaller than the optical gap by ~ 0.3 eV. If one could obtain a pure P_{2_1}/a structure, the smaller thermal gap should be detectable by electrochemical experiments or work-function measurements.

A check on our calculated band structure is afforded by comparison with optical-absorption spectra. Of course, the band gap has been chosen to obtain agreement with these spectra. It is significant, however, that higher-energy features of the optical absorption are well accounted for by our calculated structure, incorporating the self-energy correction. Because of the small dispersion of bands 35 and 36, the ones just below the valence-band edge, and of bands 41 and 42, just above the conduction-band edge, they have quite high densities of states. As a result, optical transitions between these bands should lead to a relatively narrow, high-intensity absorption peak. This peak has been identified as the one showing high absorption above 5.5 eV, and reaching a maximum at 6 eV.[36] The 1D band-structure calculations of Duke and Ford[4] lead to a value of 6.5 eV for the absorption due to this peak. Our single-chain structure leads to this result also. The calculation of Shuai, Beljonne, and Bredas[5] leads to a value of 6.9 eV for this absorption. However, our 3D band-structure calculations lead to lower-energy transitions. For P_{2_1}/n, in particular, transitions as low in energy as 5.5 eV are found. Also, whereas the 1D calculations give widths ~ 0.05 eV for this absorption band, the width from the 3D calculation is of the order of an eV, in apparent agreement with experiment.

A third and broader absorption starting at 4.5 eV has been identified by Bradley[36] as due to transitions between one of the flat bands and the conduction- or valence-band edge, specifically between bands 35 or 36 and the conduction-band edge 39 or 40, or between the valence-band edge 37 or 38 and bands 41 or 42. According to Figs. 8 and 9, such transitions would start at ~ 4 eV and extend past 6 eV, in better agreement with experimental data than the 1D band-structure results.[36] We conclude that the shift chosen to correct the LDA calculations, and the resulting band structures of Figs. 8 and 9, are in good agreement with experiment.

It is apparent from Figs. 8 and 9 that the effective mass varies greatly with direction. The small interchain coupling leads to a lack of dispersion and very large masses for $\mathbf{k}$ vectors in the directions BD, ΓY, ΓX, and AE, for example. The smallest mass is obtained for $\mathbf{k}$ in the chain direction, where there is maximum dispersion. For the chain direction we find electron and hole masses to be $\sim 0.1 m_e$, where m_e is the free-electron mass. Effective masses intermediate between this value and the very large values for the directions specified above are found for $\mathbf{k}$ along ΓB and DX, for example.

To get some idea of the effects of ring rotation out of the plane of the backbone we did calculations for P_{2_1}/a of the band structure with the rings in the two chains of the unit cell twisted relative to each other. Specifically, we calculated for two configurations in which each ring was twisted 7°, in one case toward each other so as to minimize the C-H distance, in the other away from each other so as to maximize this distance. In the former case the uncorrected gap between bands 38 and 39 at B was increased by 0.11 eV, while in the latter it was decreased by less than 0.01 eV. The uncorrected gap at Δ was increased by 0.05 eV in the former case, 0.03 in the latter case. Reflecting the changes in C-H distance, the splitting at B between bands 38 and 39 was increased in the former case from 0.41 to 0.43 eV, while in the latter case it decreased to 0.38 eV.

We conclude that the gap changes due to the twist, found to be $\sim 7°-10°$ at room temperature,[16] are not significantly greater than the errors in our calculation. The temperature-dependent libration would result at 300 K in the gap varying by ~ 0.1 eV during the period of the libration. This would be seen as a broadening of the absorption edge and the luminescence.

D. Wave functions

Because the wave functions of the top valence bands and lowest conduction bands are predominantly π, little

information about them is obtained by plotting them in the plane of the backbone. Therefore, we have plotted them in planes perpendicular to the backbone and in a plane parallel to the plane of one of the chains but removed from it by 0.75 Å. Note also that we have plotted $|\Psi\Psi^*|$ rather than the wave functions, which are complex. In Fig. 12(a) we show the charge density of the top valence band, No. 38, for P_{2_1}/a at B, D, and Δ, the points we have found to be at or close to the top of the valence band. Significantly the charge density was found to be the same at these three points. The plane at 0.75 Å has been chosen parallel to the plane of the chain at the bottom of the figure. It is seen that, as expected, for the highest valence band the charge density is spread over the monomer, thus delocalized over the entire chain. The largest density is in the double bond of the vinylene group. By virtue of the setting angle Φ_s being 52° (see Fig. 2), the chosen plane is not far from being perpendicular to the backbone of the other chain in the unit cell. (Actually, the angle of the plane with the backbone is 76° rather than 90°.) Thus the chain at the top of Fig. 12(a) shows the p-type character of the charge density, specifically its vanishing in the plane of the backbone and its symmetry about that plane.

The distribution of the charge density over the atoms varies, of course, with $|\mathbf{k}|$. At Γ, as shown in Fig. 12(b), the charge in the highest valence band No. 38 is still more strongly concentrated on the double bond and quite weak on the ring. The charge density of the lowest conduction band No. 39 at B, D, and Δ is quite different from that of the highest valence band at those points. Figure 12(c) shows it to be concentrated on those bonds where it is least concentrated in band 38. As with band 38, the charge is quite delocalized, accounting for the sizable bandwidth.

The charge density for one of the next-lower pair of valence bands, No. 36, is seen in Fig. 12(d) to be totally concentrated on the rings. As pointed out by Bradley,[36] the negligible charge density at the paraposition of the ring does not allow significant hybridization of the phenylene and vinylene π states. The localized nature of the state results in the very small bandwidth seen in Figs.

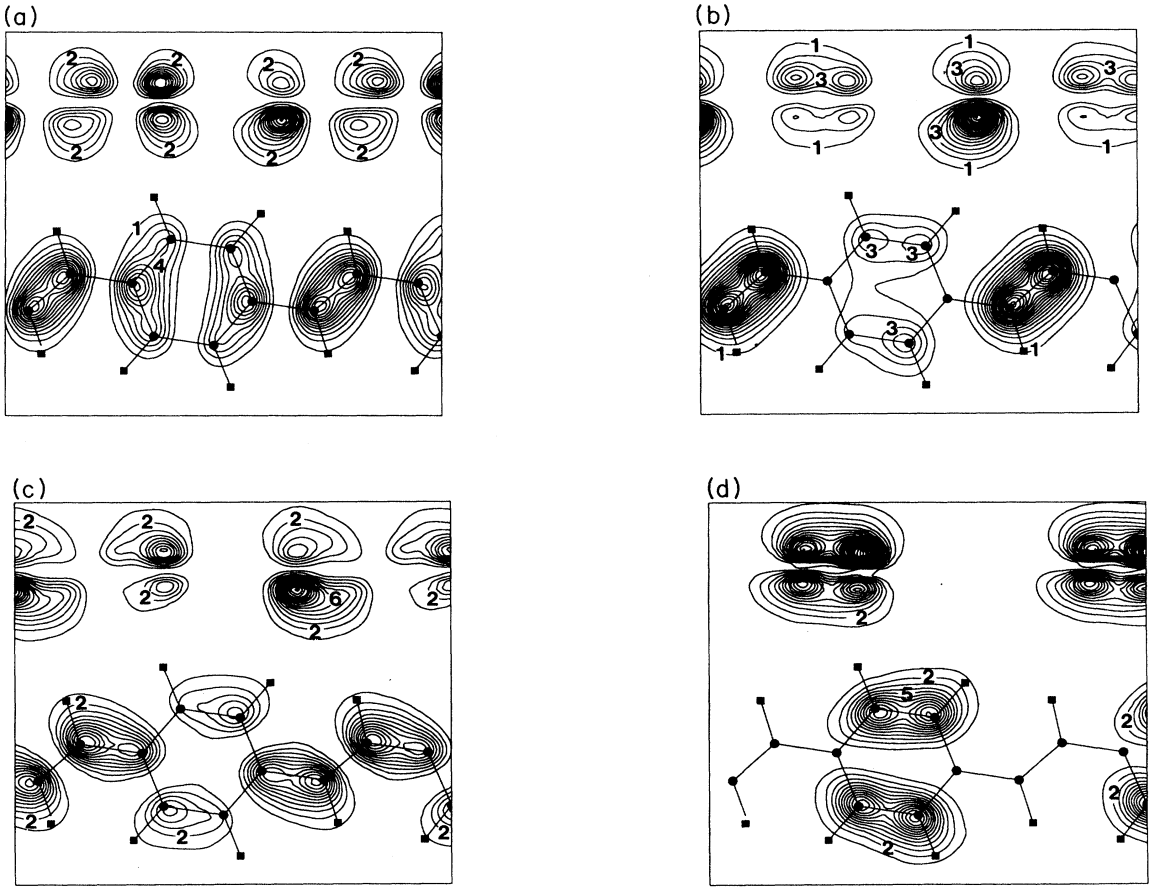

FIG. 12. Charge densities in the unit cell of P_{2_1}/a for a plane parallel to and removed 0.75 Å from the backbone of the chain at the bottom of the figure for (a) the highest valence band, No. 38, at B, D, and Δ; (b) the highest valence band, No. 38, at Γ; (c) the lowest conduction band, No. 39, at B, D, and Δ; (d) the valence band No. 36 (flat band) at Δ. The straight lines joining atoms are a guide for the eye.

8–10. From the charge density on the other chain in the unit cell, at the top of Fig. 12(d), it is seen that the wave function has mainly, if not entirely, π symmetry.

E. Comparison with 1D band structure

It is of interest to compare our results for energy vs **k** in the chain direction with the π bands obtained by 1D calculations of the band structure. The four π bands can be picked out of the valence bands found in our single-chain calculation as the bands that have vanishing wave functions in the plane of the backbone. These bands are marked by dashes in Fig. 10. In the top π band the energy E should increase from its value at Γ, initially as $\mathbf{k}^2$, reaching its maximum at $\pm\pi/c=\pm 0.477/\text{Å}$. The distance ΓP in the Brillouin zone is 0.681 Å. Thus E should reach its maximum value at $0.477/0.681=0.7$ of the distance ΓP in the zone. This point has been denoted Δ in Figs. 7–10. It is seen that E does reach its maximum at the point Δ. The difference in energy between Γ and Δ, which corresponds to the 1D bandwidth, is 2.48 eV for the top valence band [highest occupied molecular orbital (HOMO)] in $P2_1/a$, 2.42 eV in $P2_1/n$. That is only slightly larger than the 1D bandwidths of ~ 2 and 2.3 eV obtained in Refs. 4 and 5, respectively. The other three predominantly π bands between Γ and Δ in $P2_1/a$ and $P2_1/n$ are easily picked out because they are quite similar to the π bands shown in Fig. 10. This, in fact, indicates that the 3D calculation gives quite similar results to a 1D calculation for energy of the valence bands vs **k** along the chain direction. The good agreement of our results with those obtained in Refs. 4 and 5 is also seen for the other three π bands, with the exception of the second-lowest π band in Ref. 5. The latter was found in that calculation to have increasing energy with increasing **k**, whereas according to our calculations (see Fig. 10) and those of Ref. 4, it has decreasing energy with increasing **k**. We judge that this result in Ref. 5 is in error.

V. CONCLUSIONS

A. Effect of interchain coupling on band structure

In summary, the effects of interchain coupling on the band structure of PPV are (1) the top valence bands and lowest conduction bands show deviations from the pure π symmetry found in the single-chain calculation. More important, the wave functions of these band-edge states are no longer confined to the carbons but include bonds to the hydrogens on the rings; (2) the double degeneracy of the bands that would exist if the two chains in the unit cell were uncoupled is split, by up to 0.4 eV, at various points in the Brillouin zone; (3) electron-hole symmetry is lost; (4) the valence-band edge lies between the points B and D, close to B for $P2_1/a$, to D for $P2_1/n$. For $P2_1/a$ we find a thermal gap that is less than the optical gap by 0.3 eV; (5) the difference in total energy of $P2_1/a$ and $P2_1/n$ is small and it is possible that both space groups exist in different parts of the samples that are currently available; (6) the 3D gap is smaller than the 1D gap by 0.2 eV; (7) the locations and widths of the (mainly) π bands obtained from the 3D calculation are sufficiently different from those of the π bands obtained in the 1D calculation that the 3D calculation gives much better agreement with the optical absorption beyond the band edge once the upward shift of the conduction band is made; (8) taking the splitting of the bands at a band edge due to the interchain interaction as $4t_\perp$, we find $t_\perp \simeq 0.08$ eV for $P2_1/a$, 0.06 eV for $P2_1/n$. Since the average C-C spacing is about the same as in polyacetylene, we take $t_\parallel = 2.5$ eV, the value for that case. Thus the ratio $(t_\perp/t_\parallel) \simeq 0.03$ for PPV. The value of $(t_\perp/t_\parallel)$ for polyacetylene obtained by Vogl and Campbell[13] is $\simeq 0.05$.

B. Effect of interchain coupling on polarons

The effect of interchain coupling on polaron stability was investigated for the case of Holstein-model polarons by Gartstein and Zakhidov[10] and Emin.[11] These authors found that stability of a polaron requires $(t_\perp/t_\parallel) \leq 0.01$. A similar condition should hold for the polarons in conjugated polymers. This suggests that stable polarons would not exist in perfect crystals of PPV or polyacetylene. Indeed, as noted earlier, the calculations of Vogl and Campbell showed that addition of an electron to a chain in a 3D polyacetylene lattice did not result in a localized level unless an unreasonably large lattice distortion was assumed.[12,13] With $t_\perp/t_\parallel$ about the same as that for polyacetylene, perfect PPV should not have stable polarons either. In that case an electron or hole placed on a PPV chain would act like a free electron or hole in a 3D semiconductor; there would be no lattice distortion.

Of course, currently made polymers are hardly perfect; they have many defects. It has been usual, as discussed earlier, to interpret experiments in which an electron or hole is added to a polymer chain in terms of polaron creation, but direct evidence for the existence of polarons has been elusive. Exceptions are moderately doped polypyrrole[37] and poly(3-hexyl thienylene) where the charges were introduced by injection.[38] In both cases the polarons were identified by the presence of three optical-absorption bands within the gap rather than the two characteristic of bipolarons. It is noteworthy that interchain coupling was particularly weak or ineffective in these two cases, in the former because the polypyrrole was amorphous, in the latter because of the long-hexyl side groups that keep the chains apart.

Polarons have been detected on doped oligomers of PPV. Solid-state electron-nuclear double resonance (ENDOR) experiments were carried out on PPV oligomers containing three to seven phenyls and singly charged by previous exposure to Li in THF.[39] These experiments revealed that the length of the polaron, or more accurately the length of its spin-density distribution, increased with the length of the oligomer (although extrapolating to a finite length for an infinite chain). Also, the spin-density distribution was quite different for oligomers with even and odd numbers of phenyls.[39]

A PPV sample with inclusions of unconverted precursor polymer, or other defects which break the conjugation, might be thought of as an assembly of oligomers.

Putting an electron or a hole on such oligomers by doping or by above-band-gap light polarized perpendicular to the chains should create polarons in the same way as found in the ENDOR experiments of Brendel *et al.*[39] Evidence for such polarons was found by Sakamoto *et al.* by comparing resonant Raman spectra of PPV with those of anions and dianions of model compounds closely resembling segments of PPV with different lengths.[40] Sakamoto *et al.* found strong similarities in the spectra which led them to conclude that their PPV had three types of polarons and one type of bipolaron localized over different chain lengths. Specifically, the anions which led to similar spectra contained four, five, and six phenyls, respectively. Upon prolonged heat treatment, Sakamoto *et al.* found that the shortest polaron vanished, and new bipolarons were created. Presumably the polarons had combined to form bipolarons, which are more stable.

Thus polarons exist at least in some doped samples of PPV. Of course, the attractive charge of the dopant may act to stabilize the polaron. It is therefore necessary to consider separately whether polarons result from electrons and holes created on separate chains by photons. Whether polarons are created or the free electrons and holes persist, there is apparently a period of ~ 100 ps in which to observe them before they combine to form bipolarons or annihilate each other.[41] During this period these excitations could be observed by transient photoconductivity measurements or photoinduced absorption. The latter measurements are not yet available for PPV. From the former, specifically from the measured photocurrent and an estimate of the number of carriers, the mobility μ of the excitations is obtained as 8×10^{-2} $cm^2/V\,s$.[41] This appears to be a reasonable value for polarons drifting along the chains in PPV. The value obtained, both experimentally[42] and theoretically[43] for drifting polarons in polyacetylene was 2 $cm^2/V\,s$, and polarons in PPV should have greater mass because their motion involves ring rotations. The value of 8×10^{-2} $cm^2/V\,s$ is much too low for free electrons or holes in PPV. The mobility of free electrons at the band edge scattered by phonons has been calculated as 600 $cm^2/V\,s$ for polyparaphenylene (PPP) at 300 K.[44] The mobility of electrons in PPV should be comparable. The calculation for PPP did not include ring rotation, but this effect could not reduce the mobility by a factor greater than 10^3.

We note that with the large $t_\perp/t_\parallel$ making the existence of the polaron dependent on defects, the geometry and energy levels of such polarons as exist must be quite dependent on local crystal conditions. Because these conditions could be expected to vary widely over the crystal, the polaron absorption should be broad, relatively featureless, and possibly even varying from sample to sample. These features were found in the photoinduced absorption of polyacetylene under conditions where the excitations should be essentially all electrons and holes or polarons, i.e., 10–300 ps after a light pulse with polarization perpendicular to the chains.[45] It would be difficult to account for such absorption with free electrons or holes.

ACKNOWLEDGMENTS

We are grateful to J. L. Martins for the use of his norm-conserving nonlocal pseudopotential for carbon. One of us (P.G.C.) acknowledges the support of NSF Grant No. CHE-9120001 and the NSF supercomputer time, Grant No. DMR910024P, used at the Pittsburgh Supercomputer Center.

[1]T. Granier, E. L. Thomas, D. R. Gagnon, and F. E. Karasz, J. Polym. Sci., Polym. Phys. Ed. **24**, 2793 (1986).

[2]J. H. Burroughes, D. D. C. Bradley, A. R. Brown, R. N. Marks, K. Mackay, R. H. Friend, P. L. Burn, and A. B. Holmes, Nature **347**, 539 (1990).

[3]J. L. Brédas, R. R. Chance, R. H. Baughman, and R. Silbey, J. Chem. Phys. **76**, 3673 (1982).

[4]C. B. Duke and W. K. Ford, Int. J. Quantum Chem., Quantum Chem. Symp. **17**, 597 (1983).

[5]Z. Shuai, D. Beljonne, and J. L. Brédas, Solid State Commun. **78**, 477 (1991).

[6]J. B. Schlenoff, J. Obrzut, and F. E. Karasz, Phys. Rev. B **40**, 11 822 (1989).

[7]R. H. Friend, D. D. C. Bradley, and P. D. Townsend, J. Phys. D **20**, 1367 (1987).

[8]Z. Vardeny, E. Ehrenfreund, O. Brafman, M. Nowak, H. Schaffer, A. J. Heeger, and F. Wudl, Phys. Rev. Lett. **56**, 671 (1986).

[9]F. L. Pratt, K. S. Wong, W. Hayes, and D. Bloor, J. Phys. C **20**, L41 (1987).

[10]Yu. N. Gartstein and A. A. Zakhidov, Solid State Commun. **60**, 105 (1986).

[11]D. Emin, Phys. Rev. B **33**, 3973 (1986).

[12]P. Vogl and D. K. Campbell, Phys. Rev. Lett. **62**, 2012 (1989).

[13]P. Vogl and D. K. Campbell, Phys. Rev. B **41**, 12 797 (1990).

[14]D. D. C. Bradley, A. R. Brown, P. L. Burn, J. H. Burroughes, R. H. Friend, A. B. Holmes, K. D. Mackay, and R. N. Marks, Synth. Met. **43**, 3135 (1991).

[15]H. Eckhardt, K. Y. Jen, L. W. Shacklette, and S. Lefrant, in *Conjugated Polymeric Materials: Opportunities in Electronics, Optoelectronics and Molecular Electronics,* edited by J. L. Brédas and R. R. Chance (Kluwer, Dordrecht, 1990), p. 305

[16]D. Chen, M. J. Winokur, M. A. Masse, and F. E. Karasz, Polymer (to be published).

[17]D. Chen, M. J. Winokur, M. A. Masse, and F. E. Karasz, Phys. Rev. B **41**, 6759 (1990).

[18]T. Granier, E. L. Thomas, and F. E. Karasz, J. Polym. Sci., Polym. Phys. Ed. **27**, 469 (1989).

[19]M. A. Masse, D. C. Martin, E. L. Thomas, F. E. Karasz, and J. H. Petermann, J. Mater. Sci. **25**, 311 (1990).

[20]H. Matoussi and F. E. Karasz (unpublished).

[21]P. Hohenberg and W. Kohn, Phys. Rev. **136**, B284 (1964).

[22]W. Kohn and L. J. Sham, Phys. Rev. **140**, A1133 (1965).

[23]D. R. Hamann, M. Schlüter, and C. Chiang, Phys. Rev. Lett. **43**, 1494 (1979).

[24]J. Ihm, A. Zunger, and M. L. Cohen, J. Phys. C **12**, 4409 (1979).

[25]N. Trouillier and J. L. Martins, Solid State Commun. **74**, 613 (1990); Phys. Rev. B **43**, 1993 (1991).

[26]D. J. Chadi and M. L. Cohen, Phys. Rev. B **8**, 5747 (1973); H.

J. Monkhorst and J. D. Pack, *ibid.* **13**, 5188 (1976).
[27]J. E. Dennis, Jr. and J. J. Moré, SIAM Rev. **19**, 46 (1977).
[28]P. Bendt and A. Zunger, Phys. Rev. B **26**, 3114 (1982).
[29]D. M. Ceperly and B. I. Alder, Phys. Rev. Lett. **45**, 566 (1980).
[30]J. P. Perdew and A. Zunger, Phys. Rev. B **23**, 5048 (1981).
[31]D. M. Wood and A. Zunger, J. Phys. A **18**, 1343 (1985).
[32]W. P. Su, J. R. Schrieffer, and A. J. Heeger, Phys. Rev. B **22**, 2099 (1980). For a general reference on the Hückel technique see, for example, L. Salem, *Molecular Orbital Theory of Conjugated Systems* (Benjamin, New York, 1966).
[33]R. W. Godby, M. Schlüter, and L. J. Sham, Phys. Rev. Lett. **56**, 2415 (1986).
[34]M. S. Hybertsen and S. G. Louie, Phys. Rev. B **34**, 5390 (1986).
[35]G. A. Baraff and M. Schlüter, Phys. Rev. B **30**, 3460 (1984).
[36]D. D. C. Bradley, J. Phys. D **20**, 1389 (1987).
[37]J. L. Brédas, J. C. Scott, K. Yakushi, and G. B. Street, Phys. Rev. B **30**, 1023 (1984).
[38]K. E. Ziemelis, A. T. Hussain, D. D. C. Bradley, and R. H. Friend, Phys. Rev. Lett. **66**, 2231 (1991).
[39]P. Brendel, A. Grupp, M. Mehring, R. Schenk, K. Müllen, and W. Huber, Synth. Met. **45**, 49 (1991).
[40]A. Sakamoto, Y. Furukawa, and M. Tasumi, J. Phys. Chem. (to be published).
[41]D. D. C. Bradley, Y. Q. Shen, H. Bleier, and S. Roth, J. Phys. C **21**, L515 (1988).
[42]M. Sinclar, D. Moses, and A. J. Heeger, Solid State Commun. **59**, 343 (1986).
[43]E. M. Conwell and S. Jeyadev, Mol. Cryst. Liq. Cryst. **160**, 443 (1988).
[44]C. Menendez and F. Guinea, Phys. Rev. B **28**, 2183 (1983).
[45]L. Rothberg, T. M. Jedju, P. D. Townsend, S. Etemad, and G. L. Baker, Phys. Rev. Lett. **65**, 100 (1990).